

# Organic & Biomolecular Chemistry

Accepted Manuscript



This is an *Accepted Manuscript*, which has been through the Royal Society of Chemistry peer review process and has been accepted for publication.

*Accepted Manuscripts* are published online shortly after acceptance, before technical editing, formatting and proof reading. Using this free service, authors can make their results available to the community, in citable form, before we publish the edited article. We will replace this *Accepted Manuscript* with the edited and formatted *Advance Article* as soon as it is available.

You can find more information about *Accepted Manuscripts* in the [Information for Authors](#).

Please note that technical editing may introduce minor changes to the text and/or graphics, which may alter content. The journal's standard [Terms & Conditions](#) and the [Ethical guidelines](#) still apply. In no event shall the Royal Society of Chemistry be held responsible for any errors or omissions in this *Accepted Manuscript* or any consequences arising from the use of any information it contains.

## ARTICLE

# Physicochemical Studies on the Copper(II) Binding by Glycated Collagen Telopeptides

Cite this: DOI: 10.1039/x0xx00000x

Meder Kamalov,<sup>a</sup> Paul W.R. Harris,<sup>b</sup> Christian G. Hartinger,<sup>a</sup> Gordon M. Miskelly,<sup>a</sup> Garth J. S. Cooper<sup>b,c,d</sup> & Margaret A. Brimble\*<sup>a,b</sup>Received 00th January 2012,  
Accepted 00th January 2012

DOI: 10.1039/x0xx00000x

www.rsc.org/

Emerging evidence indicates that levels of advanced glycation end-products (AGEs) correlate with age- and diabetes-related organ damage and may play a causative role in such damage. Increased chelation of Cu(II) ions appears to play an important role in this process, however, the precise relationship between formation of AGEs and accumulation of Cu(II) is yet to be determined. The interaction between AGEs and Cu(II) has been investigated using a collagenous peptide that has been site-specifically modified by a key AGE. Potentiometric titration showed that introduction of this AGE increased the capacity of the host-peptide to bind Cu(II). This result was confirmed by mass spectrometric characterisation of the AGE-modified peptide-Cu(II) system.

## Introduction

Divalent copper is an integral component of cuproproteins. These proteins serve a number of physiological functions that are critical for the growth, development, and fitness of the human organism.<sup>1</sup> A prolonged severe imbalance in Cu(II) metabolism leads to serious debilitating conditions, such as Menkes disease in cases of Cu(II) deficiency and Wilson's disease in cases of Cu(II) excess.<sup>2,3</sup> An imbalance in Cu(II) metabolism on a smaller scale is also believed to play an important role in the pathogenesis of a number of ageing- and diabetes-related conditions.<sup>4</sup> The precise cause and effects of this imbalance are yet to be determined.

Elevated levels of chelatable Cu(II) in tissues are observed in nonclinical models of diabetes, whereas studies of urinary copper excretion have provided evidence for systemic copper excess in diabetic patients.<sup>4</sup> Because Cu(II) is highly redox active it can contribute to diabetic tissue damage by generating reactive oxygen species.<sup>5</sup> The mechanism by which diabetes and the resulting hyperglycaemia lead to tissue Cu(II) excess remains unresolved.

This disbalance in the metabolism of Cu(II) could be mediated by advanced glycation end-products (AGEs). AGEs are a family of derivatives of naturally occurring amino acids that form when sugars and sugar degradation products modify protein side-chains.<sup>6</sup> Such AGE formation is irreversible and AGE-modification of proteins in blood-vessel walls is a widespread phenomenon in diabetes. AGE accumulation is closely linked to the pathogenesis of vasculopathy and organ damage in nonclinical models and in diabetic patients.<sup>6</sup> Levels of AGEs and the extent of disbalance of Cu(II) metabolism both increase with the advanced age and increase markedly with the onset of diabetes mellitus.<sup>7,8</sup>

The relationship between AGEs and Cu(II) appears to lead to a self-reinforcing and destructive cycle. Treatment of diabetic rats with a copper chelator has significantly reduced

the levels of not only Cu(II) but also of AGEs and AGE-precursors.<sup>9</sup> This result is consistent with the concept that excess Cu(II) plays an important role in AGE formation. AGEs, in turn, are believed to produce the pathological Cu(II)-binding sites in tissues, thus further enhancing the systemic excess of Cu(II). Yet direct evidence for Cu(II)-binding by protein-bound AGEs is missing.<sup>10</sup>

A key member of the AGE family, N<sup>ε</sup>-carboxymethyllysine (CML, Fig. 1), accumulates in organ tissues and its levels correlate with the severity of ageing-related conditions, such as cataract and heart disease.<sup>11</sup> Because of its structure, CML has the potential to effectively chelate Cu(II) ions via the N-donor atom (the ε-amine) and the neighbouring carboxylate.<sup>12</sup> However, the effect of CML formation on the overall metal binding capacity of a host peptide or protein has not been reported.

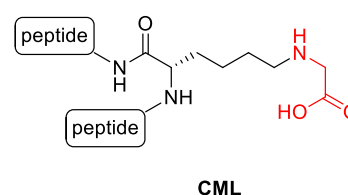


Fig. 1 Peptide-bound CML

Peptide complexes of metal ions have been extensively investigated as model systems for metalloprotein structure and function.<sup>13</sup> Herein we report our initial studies on the Cu(II) binding properties of peptides site-specifically modified by CML. Since collagen is the major target of glycation and the telomere region of collagen has access to transition metals *in vivo*,<sup>14,15</sup> modified collagen telopeptides were employed as glycation targets.

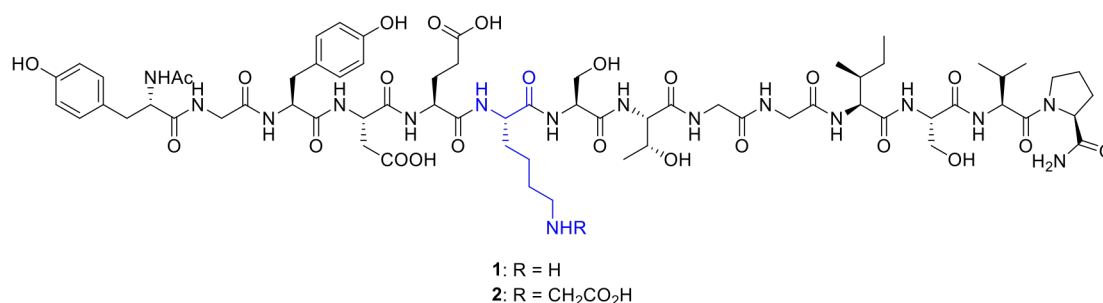


Fig. 2 Structures of the target peptides 1 and 2

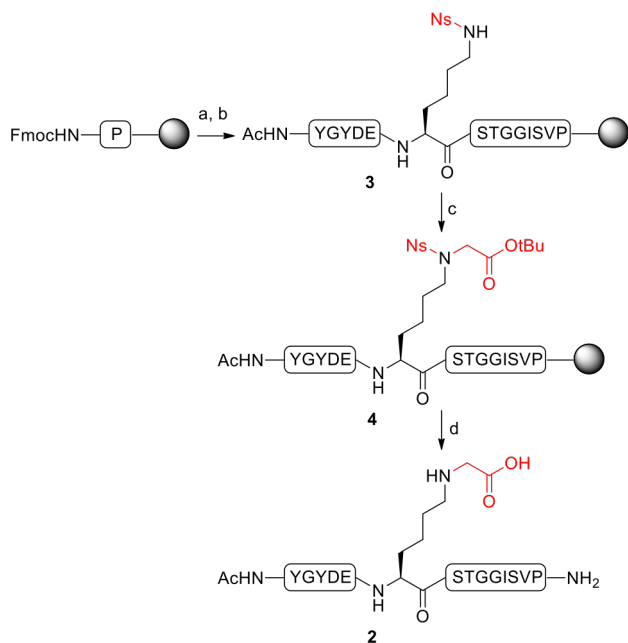
## Results and discussion

### Peptide synthesis

The binding behaviour between peptides 1 and 2 (Fig. 2) as ligands and Cu(II) was investigated via potentiometry and mass spectrometry.

The peptide sequence YGYDEKSTGGISVP was used to model the telomere region of collagen and was derived from human type I  $\alpha 1$  collagen.<sup>16</sup> Peptide 1 was synthesised via automated solid phase peptide synthesis following the procedure described previously.<sup>17</sup> Peptide 2 was synthesised via

an on-resin amino alkylation strategy,<sup>18</sup> where Fmoc-Lys(Ns)-OH was incorporated using analogous conditions as for peptide 1 (Scheme 1). Upon completion of the assembly of peptide 3 but prior to its cleavage, the N-terminus of the resin-bound peptide was acetylated with acetic anhydride, and the resulting peptide was subjected to alkylation with *tert*-butyl bromoacetate in the presence of DIPEA to afford peptide 4. The nosyl group on peptide 4 was then smoothly deprotected using 2-mercaptoethanol and DIPEA (15 min),<sup>19</sup> and the resulting peptide cleaved from the resin with TFA-TIS-H<sub>2</sub>O (38:1:1). The crude peptide was purified by HPLC to afford 2 in 30% overall yield with >98% purity.



**Scheme 1** Synthesis of CML-containing peptide 2. *Reagents and conditions:* (a) Fmoc-SPPS *i.* 20% piperidine in DMF, *ii.* Fmoc-AA-OH, HBTU, DIPEA; *iii.* steps *i.* and *ii.* repeated until the desired sequence is built (b) *i.* N-terminal Fmoc removal: 20% piperidine in DMF, *ii.* Ac<sub>2</sub>O, DIPEA; (c) *tert*-butyl bromoacetate, DIPEA, DMF, rt, overnight; (d) *i.* Ns removal: 2-mercaptoethanol, DBU, DMF, rt, 15 min, *ii.* peptide release: TFA/TIS/H<sub>2</sub>O, rt, 2 h.

### Potentiometric analysis

Both peptides 1 and 2 feature carboxylic acid, hydroxyl, and amine functional groups. The protonation constants of peptides 1 and 2 were measured by potentiometrically titrating acidic solutions of peptides with NaOH (results summarised in Table 1). Peptide 1 can be considered a pentaprotic acid with five ionisable groups in the measurable pH range (2–12), *i.e.*, two acids, an amine, and the two phenol groups of tyrosine side-chains. In contrast to peptide 1, six ionisable groups are present in peptide 2, which has an additional carboxylic acid group. The protonation constants determined for these groups were in good agreement with literature data.<sup>20</sup> The presence of the extra carboxylic acid appeared to have altered the pK<sub>a</sub> values of the remaining acids in the peptide (Table 1).

Equipped with the pK<sub>a</sub> values for the individual functional groups of the peptides, we then measured the stability constants of complexes of peptides 1 and 2 with Cu(II) (summarised in Table 1). Only one species of a metal complex could be fitted to the experimental titration curve obtained for the peptide 1/Cu(II) system, *i.e.* CuH<sub>3</sub>L (Table 1). The stability constant obtained for CuH<sub>3</sub>L agrees with previously reported values for individual amino acid side-chain groups present in the peptide and shows that peptide 1 does not strongly bind Cu(II).<sup>21</sup>

The speciation diagram for the complex formation between Cu(II) and peptide 1 showed that the complexation started at pH 3, peaked at pH 5.5, but largely vanished at pH 7 due to competition by precipitation of Cu(OH)<sub>2</sub> (Figure 3A). *In vivo*, type I  $\alpha 1$  collagen, from which the telopeptide sequence was

taken, is predominantly exposed to an environment of pH ca. 7 and therefore little metal binding by telopeptide **1** is expected.<sup>22</sup>

**Table 1** Stepwise protonation constants for peptides **1** and **2** and their stability constants with Cu(II) at 298.1 K and  $I = 0.1$  M (NaCl)

	<b>1</b>	<b>2</b>
<b>H<sub>6</sub>L</b>	-	2.06(6)
<b>H<sub>5</sub>L</b>	2.23(7)	3.63(6)
<b>H<sub>4</sub>L</b>	5.93(7)	4.84(7)
<b>H<sub>3</sub>L</b>	9.30(4)	9.10(3)
<b>H<sub>2</sub>L</b>	10.29(4)	9.66(2)
<b>HL</b>	10.33(2)	10.07(6)
<b>CuH<sub>3</sub>L</b>	3.33(9)	4.01(5)
<b>CuH<sub>2</sub>L</b>	-	8.62(2)
<b>CuHL</b>	-	11.6(6)

The titration curve of the CML telopeptide **2** in the presence of Cu(II) was significantly different from that of the telopeptide **1**. Three metal complex species could be fitted to the titration curve, *i.e.*, CuHL, CuH<sub>2</sub>L, and CuH<sub>3</sub>L. The species distribution diagram indicated that the first complexation to form CuH<sub>3</sub>L started at pH >3.0 and peaked at pH 4.12, where it accounted

for 40% of all Cu(II) present in solution (Figure 3B). The complexation to form CuH<sub>2</sub>L started at pH 3.09 before the formation of CuH<sub>3</sub>L was complete and peaked at pH 5.85, where it accounted for 87% of all Cu(II) present in solution. In parallel, the third complexation to form CuHL started at pH 4.52 and was the dominant complex type at pH 8, the highest in this experiment. Importantly, at pH 7.00 the copper complexes CuH<sub>2</sub>L and CuHL accounted for 96% of all Cu(II) species present in solution, *i.e.*, the majority of the available copper was bound by the CML-modified collagen telopeptide **2**.

While the dramatic difference between the titration of peptides **1** and **2** in the presence of Cu(II) is notable, the key problem with such potentiometric studies of metal-peptide interaction is the complex nature of the equilibria under investigation. Furthermore, the information on the species formed is limited and therefore such data needs to be complemented by other characterisation methods such as mass spectrometry.

### Mass spectrometry

Electrospray ionisation-mass spectrometry (ESI-MS) was used to complement the potentiometric data. ESI-MS is perfectly suited for studies on ligand binding interactions due to the softness of the ionisation process. The interaction between Cu(II) ions and the synthetic telopeptides **1** and **2** at different pH levels was probed using ESI-MS by recording the mass spectra of peptides **1** and **2** in negative ion mode both in the absence and in the presence of Cu(II). For all ESI-MS experiments described here, the peptide concentration was 3.5–5 μM.

**Table 2** Experimental ( $m/z$ ) and theoretical ( $m/z_{\text{calc}}$ )  $m/z$  ( $z = 2$ ) values for peptides **1** and **2** and the identified Cu(II) adducts

Peptide	Adduct	$m/z$	$m/z_{\text{calc}}$
<b>1</b>	$[\mathbf{1} - 2\text{H}]^{2-}$	755.36	755.36
<b>1</b>	$[\mathbf{1} + \text{K} + \text{Cl} - 2\text{H}]^{2-}$	792.32	792.32
<b>1</b>	$[\mathbf{1} + \text{Na} + \text{Cl} - 2\text{H}]^{2-}$	784.34	784.34
<b>2</b>	$[\mathbf{2} - 2\text{H}]^{2-}$	784.35	784.35
<b>2</b>	$[\mathbf{2} + \text{Na} - 3\text{H}]^{2-}$	795.34	795.34
<b>2</b>	$[\mathbf{2} + \text{Cu} - 4\text{H} - \text{CO}_2]^{2-}$	792.82	792.82
<b>2</b>	$[\mathbf{2} + \text{Cu} - 4\text{H}]^{2-}$	814.82	814.82
<b>2</b>	$[\mathbf{2} + \text{Cu} + \text{Cl} - 3\text{H}]^{2-}$	833.81	833.81

As often observed for peptides, the negative ESI mass spectra of peptides **1** and **2** featured a number of singly and multiply charged ions due to deprotonation. The most abundant peaks were assigned to the respective doubly negative  $[\text{M} - 2\text{H}]^{2-}$  ions, and therefore this region of the mass spectrum was selected for data analysis (results summarised in Table 2). The peak at  $m/z$  755.36 in the spectrum of **1** at pH 7.3 was attributed to the  $[\mathbf{1} - 2\text{H}]^{2-}$  ion, while the peak at  $m/z$  792.32 was identified as the  $[\mathbf{1} + \text{K} + \text{Cl} - 2\text{H}]^{2-}$  ion. Analogously, the mass signal at  $m/z$  784.35 in the spectrum of **2** at pH 6.9 was attributed to the  $[\mathbf{2} - 2\text{H}]^{2-}$  ion, while the signal at  $m/z$  795.34 was assigned to the  $[\mathbf{2} + \text{Na} - 3\text{H}]^{2-}$  ion.

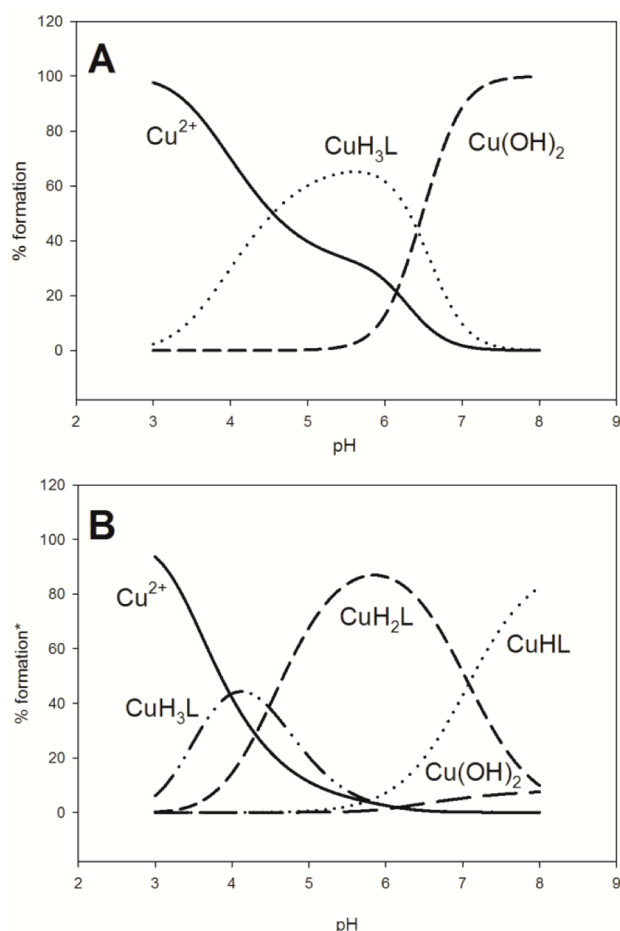


**Fig. 3** Species distribution diagrams for titration of peptides **1** (A) and **2** (B) with NaOH in presence of Cu(II)

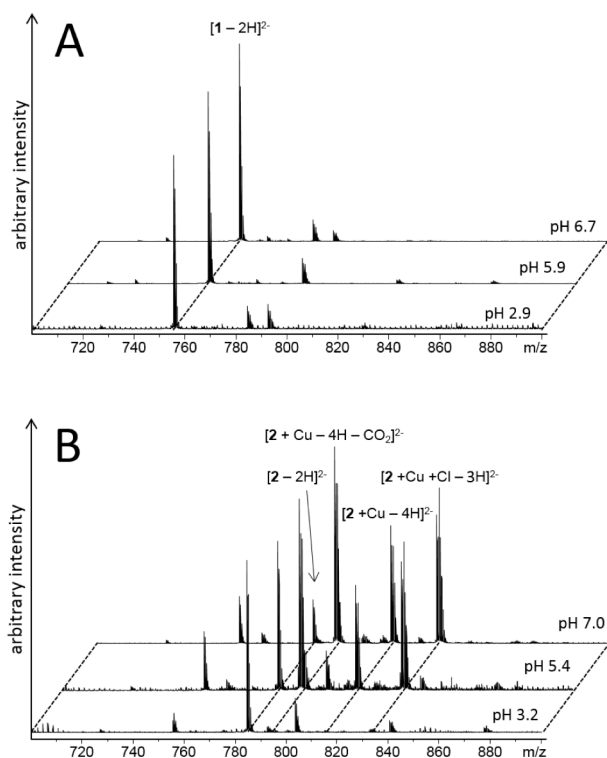


**Fig. 4** Mass spectra in the range  $m/z$  700 – 900 of peptides **1** (A) and **2** (B) in presence of Cu(II) at various pH levels featuring double negatively charged anions.

The ESI-mass spectrum of peptide **1** in the presence of Cu(II) at pH 6.7 showed no additional peaks that could be

assigned to Cu adducts but a NaCl adduct was detected at  $m/z$  784.34 (Table 2, Figure 4A). In order to study the effect of the pH on adduct formation, ESI-MS measurements of incubation mixtures containing **1** and CuCl<sub>2</sub> were conducted at pH 5.9 and 2.9. However, neither spectrum showed any evidence of Cu coordination. A KCl adduct was observed at pH 5.9, whereas at pH 2.9 both NaCl and KCl adducts were observed (Figure 4A).

Addition of CuCl<sub>2</sub> to the CML-containing peptide **2** at a molar ratio of 1:1.1 (peptide:Cu) caused the formation of ions that were not observed in the mass spectrum of **2** without CuCl<sub>2</sub> addition (Figure 4B).

Upon reaction of **2** with Cu(II) at pH 7.0 three copper containing ions were observed (Fig. 4B). The signal at  $m/z$  792.82 was assigned to the decarboxylated Cu-containing  $[2 + \text{Cu} - 4\text{H} - \text{CO}_2]^{2-}$  ion. The loss of CO<sub>2</sub> is common and can be explained by degradation of one of the three acid residues present in the system. The signal at  $m/z$  814.82 was assigned to a peptide-copper complex ion of the composition  $[2 + \text{Cu} - 4\text{H}]^{2-}$ , whereas the signal at  $m/z$  833.81 was identified as a peptide-copper complex ion of the composition  $[2 + \text{Cu} + \text{Cl} - 3\text{H}]^{2-}$ .

The mass spectrum of the CML-modified peptide **2** combined with CuCl<sub>2</sub> at pH 5.4 displayed signals corresponding to the same three peptide-copper complexes observed at pH 7.0. Notably, no adducts were observed at pH 3.2. This result is in accordance with the potentiometric titration analysis, which predicted only a small amount of copper complexation at pH 3.2.

The nature of the Cu-peptide species was further confirmed by comparing the experimentally measured isotope ratios with

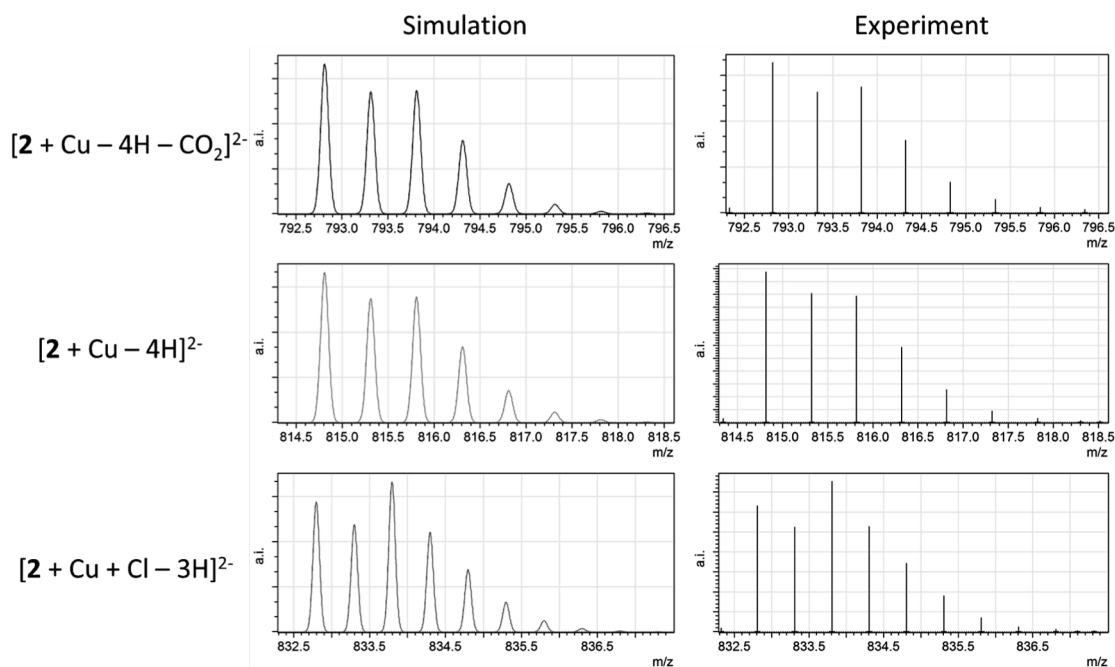


**Fig. 5** Comparison of the simulated (left) and measured (right) isotopic distributions of Cu-species observed in the mass spectra of **2** in presence of CuCl<sub>2</sub> at pH 7.0

calculated isotopic distributions (Figure 5). All of the calculated isotope distributions closely match the experimental data. The impact of the presence of Cu(II) is clearly visible in all three isotopic distributions. In case of the signal at  $m/z$  833.81 the composition was identified as  $[2 + \text{Cu} + \text{Cl} - 3\text{H}]^{2-}$ , as the isotope distribution clearly shows the presence of a single Cl in the dianion.

The results of this ESI-MS study of the copper binding by telopeptides **1** and **2** confirm the conclusions from the potentiometric study. The formation of strong copper-peptide **2** complexes was predicted by the potentiometric titration. Such Cu(II) complexes were clearly visible in the ESI-MS spectra of solution containing peptide **2** and Cu(II) at pH 7. ESI-MS measurements at lower pH levels were also in agreement with the potentiometric predictions. Thus, at pH 3.2 no copper-containing species could be observed by ESI-MS. Not surprisingly, analogous ESI-MS investigations of the lysine-containing CTP **1** did not show any copper-containing species.

## Experimental

### Peptide Synthesis

SPPS was performed via the Fmoc strategy on Rink Amide resin using a Biotage Alstra peptide synthesiser on 0.1 mmol scale. The Fmoc group was deprotected with 20% piperidine in DMF for 2 + 3 minutes at 60 °C. The coupling step was performed with Fmoc-AA-OH (5 equiv) in DMF (0.2 M), HBTU in DMF (4.5 equiv, 0.45 M) and DIPEA (10 equiv) for 5 min at 75 °C. The final Fmoc-group was removed and the amine was acetylated by Ac<sub>2</sub>O in the presence of DIPEA at rt for 10 min.

Resin-bound peptide **3** (0.1 mmol, 1 equiv) was swollen in dichloromethane (30 min), then in DMF (10 min), and drained. A solution of *tert*-butyl bromoacetate (70 µl, 0.5 mmol, 5 equiv) with DIPEA (175 µl, 1 mmol, 10 equiv) in DMF (5 ml) was added in one portion and the reaction mixture shaken overnight at rt to afford the peptide **4**, which was washed with DMF. Peptide **4** (0.1 mmol, 1 equiv) was next swollen in dichloromethane (30 min), then in DMF (10 min) and filtered. A solution of 1,8-diazabicyclo[5.4.0]undec-7-ene (90 µl, 0.6 mmol, 6 equiv) and 2-mercaptoethanol (42 µl, 0.6 mmol, 6 equiv) in DMF (5 ml) was added in one portion and the mixture shaken for 15 min, drained, and washed with DMF.

The peptides were released from the resin with concomitant removal of the side-chain protecting groups by treatment with TFA/TIS/H<sub>2</sub>O (38:1:1, 5 ml) at rt for 2 h. Peptides were precipitated with cold diethyl ether, isolated by centrifugation, washed in cold diethyl ether, dissolved in 1:1 MeCN/H<sub>2</sub>O containing 0.1% TFA and lyophilised. The peptides were analysed for purity by LCMS using a Zorbax C3 column (3.5 µ; 3 x 150 mm; Agilent) at 0.3 ml/min using a linear gradient. The solvent system used was A (0.1% formic acid in H<sub>2</sub>O) and B (0.1% formic acid in acetonitrile). Purification of the crude peptides was performed by semipreparative HPLC using a Gemini C18 column (10 µ; 250 x 10 mm; Phenomenex) at 5

ml/min using a shallow linear gradient. The solvent system used was A (0.1% TFA in H<sub>2</sub>O) and B (0.1% TFA in acetonitrile). The resulting purified peptides were analysed by the LCMS system used for crude peptide analysis. The purities were determined from the integrated areas of the peaks corresponding to peptide **1** (13.1 min) and to peptide **2** (12.7 min).

### Potentiometry

Stock solutions of supporting electrolyte, CuCl<sub>2</sub>, and peptide ligands were prepared volumetrically from the analytical grade salts. Stock solutions of HCl and carbonate-free NaOH were prepared from aqueous concentrates, and their concentrations determined by titrating the base against a volumetrically prepared potassium hydrogen phthalate standard solution. The acid was titrated against the base.

The titration apparatus consisted of a 20 mL water-jacketed glass titration vessel attached to a thermostated water bath and sitting on a magnetic stir plate. The burette and electrode were clamped to the stir plate and attached to the Metrohm Titrando 907 titrator.

The ionic strength of all solutions was set at 0.1 M using NaCl. CuCl<sub>2</sub> was the source of the metal ion. 0.01 M HCl was used in calibration of the pH electrode ( $E^{\circ} = 408.9$  V, slope factor = 0.995). Peptides **1** and **2** were dissolved in 0.01 M HCl at 0.1 M ionic strength and titrated with 0.189 M NaOH either with or without addition of the CuCl<sub>2</sub> solution. The metal-to-ligand molar ratio in titrations in the presence of Cu(II) was 1:1. Titrations were carried out under a nitrogen atmosphere at 298 K using a total volume of 5-6 ml. 0.4-0.6 mM ligand concentration was used in all measurements. Starting with the fully equilibrated initial titration solution (pH 2-3, 25°C), a known volume of base was added and the solution allowed to re-equilibrate. The potential was then recorded. This procedure was repeated until the full pH range of interest was covered.

Stability constants ( $\log \beta$ ) were determined from the potentiometric data by using *Hyperquad*.<sup>23</sup> The species distribution diagrams were prepared from the determined  $\log \beta$  values using HySS.<sup>24</sup>

### Mass spectrometry

All mass spectra were collected with a Bruker microTOF mass spectrometer (Bruker Daltonics GmbH, Bremen, Germany). A syringe pump (KD Scientific) provided a stable liquid flow at 3 µl/min to the fused silica spray capillary. This capillary protruded a short distance from the end of a stainless steel tube, through which nitrogen gas was passed to assist in desolvation. The spray assembly was held at a potential of 3.2 kV to induce charging of the liquid droplets, which were directed through a series of heated apertures into a vacuum chamber (dry gas 6 L/min, dry temperature 180 °C). Here they were desolvated to form isolated ions, which were directed by lenses into the high vacuum region of the time-of-flight mass analyser. All  $m/z$  values reported here correspond to the most

prominent mass ions within each isotopic cluster, and all calculated ion masses are based on the monoisotopic atomic weights. Peptide concentrations in the analysed solutions were 4–5  $\mu\text{M}$  and ligand-to-metal ratio was 1:1.1. Lowering of the pH was accomplished by addition of conc. acetic acid. Spectra were recorded in negative mode over 1.4 min and averaged.

## Conclusions

The majority of plasma Cu(II) is bound to ceruloplasmin, while the remainder is bound to albumin, transcuprein, various peptides and amino acids. It is known that diabetes mellitus causes defective copper regulation, and elevated tissue levels of chelatable copper occur in nonclinical models of diabetes.<sup>4</sup> A systemic excess of copper has also been shown in diabetic patients.<sup>22</sup>

Accumulation of AGEs is a widespread phenomenon in diabetes and this accumulation is closely linked to the pathogenesis of vasculopathy and organ damage. AGEs can modify amino acid residues in proteins of the fibrous ECM. Therefore accumulation of AGEs is believed to make the ECM proteins more susceptible to copper binding, thereby causing the disbalance of copper. However, to date no evidence of the enhanced copper binding by AGE-modified peptides has been reported.

Our investigation of the copper binding capacities of peptides **1** and **2** has for the first time provided direct evidence for the increased copper chelation properties of glycosylated peptides. The results of the potentiometric studies were confirmed by pH dependent ESI-MS experiments.

These results warrant further investigations into properties of AGE-copper complexes and their impact on the development of diabetic complications. One such study, an investigation of the redox properties of complexes of Cu(II) with various AGE-peptides, is currently underway.

## Acknowledgements

Authors would like to thank the Maurice Wilkins Centre for Molecular Biodiscovery for generous financial support.

## Notes and references

<sup>a</sup> School of Chemical Sciences, The University of Auckland, 23 Symonds Street, Auckland, New Zealand

<sup>b</sup> Maurice Wilkins Centre for Molecular Biodiscovery, The University of Auckland, 3 Symonds Street, Auckland, New Zealand

<sup>c</sup> School of Biological Sciences, The University of Auckland, 3 Symonds Street, Auckland, New Zealand

<sup>d</sup> Centre for Advanced Discovery and Experimental Therapeutics, Central Manchester University Hospitals, NHS Foundation Trust, and the School of Biomedicine, The University of Manchester, Manchester UK, and Department of Pharmacology, Division of Medical Sciences, University of Oxford, Oxford, UK

Electronic Supplementary Information (ESI) available: [details of any supplementary information available should be included here]. See DOI: 10.1039/b000000x/

1 T. Hirayama, G. C. Van de Bittner, L. W. Gray, S. Lutsenko and C. J. Chang, *Proc. Natl. Acad. Sci.*, 2012, **109**, 2228–2233.

2 D. J. Waggoner, T. B. Bartnikas and J. D. Gitlin, *Neurobiol. Dis.*, 1999, **6**, 221.

3 M. J. Petris, I. Voskoboinik, M. Cater, K. Smith, B. E. Kim, R. M. Llanos, D. Strausak, J. Camakaris and J. F. B. Mercer, *J. Biol. Chem.*, 2002, **277**, 46736–46742.

4 G. J. S. Cooper, *Curr. Med. Chem.*, 2012, **19**, 2828–2860.

5 J. F. Mead and W. A. Pryor, *Acad. N. Y.*, 1976, 51–68.

6 M. Hellwig and T. Henle, *Angew. Chem. Int. Ed.*, 2014, **53**, 10316–10329.

7 N. Kawamura, T. Ookawara, K. Suzuki, K. Konishi, M. Mino and N. Taniguchi, *J. Clin. Endocrinol. Metab.*, 1992, **74**, 1352–1354.

8 D. Konukoğlu, G. D. Kemerli, T. Sabuncu and H. H. Hatemi, *Horm. Metab.*, 2002, **34**, 367.

9 Y. Hamada, E. Nakashima, K. Naruse, M. Nakae, M. Naiki, H. Fujisawa, Y. Oiso, N. Hotta and J. Nakamura, *J. Diabetes Complications*, 2005, **19**, 328–334.

10 A. K. Saxena, P. Saxena, X. Wu, M. Obrenovich, M. F. Weiss and V. M. Monnier, *Biochem. Biophys. Res. Commun.*, 1999, **260**, 332–338.

11 N. Rabbani and P. Thornalley, *Amino Acids*, 2012, **42**, 1087–1096.

12 S. T. Seifert, R. Krause, K. Gloe and T. Henle, *J. Agric. Food Chem.*, 2004, **52**, 2347–2350.

13 K. L. Haas, A. B. Putterman, D. R. White, D. J. Thiele and K. J. Franz, *J. Am. Chem. Soc.*, 2011, **133**, 4427–4437.

14 J. P. Orgel, T. J. Wess and A. Miller, *Structure*, 2000, **8**, 137–142.

15 R. G. Paul and A. J. Bailey, *Int. J. Biochem. Cell Biol.*, 1996, **28**, 1297–1310.

16 M.-L. Chu, W. de Wet, M. Bernard, J.-F. Ding, M. Morabito, J. Myers, C. Williams and F. Ramirez, *Nature*, 1984, **310**, 337–340.

17 M. Kamalov, P. W. R. Harris, G. J. S. Cooper and M. A. Brimble, *Chem. Commun.*, 2014, **50**, 4944–4946.

18 M. Kamalov, S. Yang, P. W. Harris, G. J. Cooper and M. A. Brimble, *Synlett*, 2014, **25**, 1835–1838.

19 T. M. Woods, M. Kamalov, P. W. Harris, G. J. Cooper and M. Brimble, *Org. Lett.*, 2012, **14**, 5740–5743.

20 T. Kowalik-Jankowska, M. Ruta, K. Wiśniewska and L. Łankiewicz, *J. Inorg. Biochem.*, 2003, **95**, 270–282.

21 L. D. Pettit and H. K. J. Powell, *IUPAC Stability Constants Database*, Academic Software, Otley, W. Yorks, 1993.

22 G. J. S. Cooper, *Drugs*, 2011, **71**, 1281–1320.

23 P. Gans, A. Sabatini and A. Vacca, *Talanta*, 1996, **43**, 1739–1753.

24 L. Alderighi, P. Gans, A. Ienco, D. Peters, A. Sabatini and A. Vacca, *Coord. Chem. Rev.*, 1999, **184**, 311–318.